Environmental Engineering and Management Journal

February 2021, Vol. 20, No. 2, 217-227
http://www.eemj.icpm.tuiasi.ro/; http://www.eemj.eu

"Gheorghe Asachi" Technical University of Iasi, Romania

EVALUATION OF PHOSPHATE AND AMMONIUM ADSORPTION-DESORPTION OF SLOW PYROLYZED WOOD BIOCHAR

Masood Rezaee[1, 2*], Saeed Gitipour[1], Mohammad-Hossein Sarrafzadeh[2]

[1]School of Environment, College of Engineering, University of Tehran, Tehran, Iran
[2]UNESCO Chair on Water Reuse, School of Chemical Engineering, College of Engineering, University of Tehran, P.O. Box 11155-4563, Tehran, Iran

Abstract

Biochar is attracting attention as a soil amendment and organic/inorganic adsorbent for water purification. Proper use of biochar in such cases requires understanding of the mechanisms of nutrient adsorption and desorption on biochar. In this study, slow pyrolyzed wood biochar's were prepared at temperatures 400 and 600°C with retention time of 60 and 120 minutes to investigate their phosphate and ammonium adsorption capacities. The effects of pyrolysis process conditions and biochar physicochemical properties on potential adsorption capacity were evaluated. Results of adsorption kinetics showed that both pseudo-first-order and pseudo-second-order models could well predict the adsorption kinetics of phosphate and ammonium indicating that the chemical adsorption was one of the main mechanisms of phosphate and ammonium absorption. Langmuir-Freundlich isotherm was the best-fit model for ammonium adsorption which means the occurrence of chemical adsorption on heterogeneous surface whilst Langmuir isotherm agreed well with the phosphate adsorption. For different biochar's, ammonium adsorption capacity ranged from about 0.34 to 5.3 mg/g and phosphate adsorption capacity ranged from about 0.6 to 42.2 mg/g. Phosphate adsorption capacity improved with increasing temperature and retention time of pyrolysis process. However, higher ammonium adsorption which was observed in lower pyrolysis temperature and residence time can be attributed to more oxygen-containing functional groups. Both phosphate and ammonium adsorptions-desorption by biochar are more strongly related to solution pH, and maximum adsorption capacities were observed at pH of 7 and 3 for ammonium and phosphate, respectively.

Key words: adsorption, ammonium, biochar, isotherm, phosphate

Received: December, 2019; Revised final: July, 2020; Accepted: September, 2020; Published in final edited form: February, 2021

1. Introduction

Biochar, the carbon-rich solid, exhibited an extensive application due to the interesting features such as highly-porous structure, functional groups and large specific surface area (Lehmann and Joseph, 2015, Weber and Quicker, 2018). Biochar is prepared by pyrolysis as a thermochemical process which decompose biomass feedstocks by heating in the absence or low concentration of oxygen. Other products of pyrolysis process include condensable liquid (called bio-oil) and non-condensable gas. Based on the heating rate and solid retention time, the pyrolysis process is categorized into slow (conventional), fast and flash pyrolysis (Balat et al., 2009). Each of these processes is employed depending on the feedstock and the intended target. In slow pyrolysis, biomass has enough time for conversion and repolymerization reactions in order to maximize the solid product yield (Al Arni, 2018, Kan et al., 2016). The main characteristics of biochar, such as specific surface area, ash content, density, volatility, water holding capacity, porosity and pH are very sensitive to the pyrolysis process conditions and biomass feedstocks (Peng et al., 2011; Tang et al., 2013; Wei et al., 2019; Zhao et al., 2018). Wood is an attractive biomass resource because it is not considered a food source unlike many other biomass

* Author to whom all correspondence should be addressed: e-mail: masrezaee@ut.ac.ir

feedstocks (Jackson et al., 2018). In addition to forest biomass resources, wood residue can also be found in demolition waste and municipal solid waste (Liikanen et al., 2019, Paolotti et al., 2017).

There are different functional groups (nitro, chloro, hydroxyl, amine, carbonyl, carboxyl) on the surface of biochar which is strongly dependent on the type of biomass feedstock and pyrolysis condition, for example biochar derived from animal manure or sewage sludge has a higher amount of sulphur and nitrogen functional groups. Additionally, the chemistry of the carbon adsorbent surface is highly dependent on environmental conditions such as pH and can perform a variety of functions. Generally, at high pH, phenyl and carboxylic groups release protons and find a negative charge, whereas at low pH, amine functional groups adsorb the proton and find a positive charge (Fagbohungbe et al., 2017).

In recent years, the use of biochar has received widespread attention in various environmental applications including: 1) increases soil fertility and agricultural performance; 2) reduces application of pesticide and synthetic fertilizers; 3) reduces methane and nitrous oxide emissions from soil; 4) reduces chemical and nitrate leaching to catchments; 5) creating local jobs and local economic cycles (Oliveira et al., 2017, Shareef and Zhao, 2017). In addition to the environmental benefits, biochar is an attractive adsorbent from economic perspective because of the lower price compared to other adsorbents such as zeolite and activated carbon (Alhashimi and Aktas 2017, McCarl et al., 2009). A research on the performance of activated carbon and biochar for wastewater treatment and nutrient recycling showed that biochar is less obstructed because of its larger pores. As well as the residue of biochar can be used in agricultural application due to its nutrients (such as nitrogen and phosphorus) (Huggins et al., 2016).

Adsorption is essentially a dynamic process that must be balanced over time between the adsorbent and the adsorbed matter. Numerous studies have been recently reviewed biochar capacity to adsorb organic and inorganic matters. Electrostatic interactions, physical adsorption and chemical bonding (complex formation/deposition) have been identified as governing mechanisms in the adsorption of heavy metals and organic matter by biochar (Tan et al., 2015, Zhou et al., 2018, Zhu et al., 2016). Despite several studies were done about phosphate adsorption by biochar in recent years, inconsistent results have been reported. Yao et al. (2012) by investigating different biomass biochar (sugarcane bagasse, peanut hull, Brazilian pepper wood and bamboo) in different pyrolysis temperatures do not suggest specific phosphate adsorption trend. Novais et al. (2018) reported that biochar's do not have phosphate adsorption capacity without pre-treatment because of large amount of phenolic and carboxylic groups. Hollister et al. (2013) do not observed any phosphate adsorption by corn biochar. Similarly, some types of biochar such as green waste and sugarcane bagasse biochar do not have capability to adsorb phosphate and phosphate release into solution is also observed in some types (Zhang et al., 2016). However, there are several papers that report biochar capacity for phosphate adsorption. Laird et al. (2010) indicated that biochar addition could decrease phosphate leaching up to 69% in column test. Takaya et al. (2016) demonstrated that the PO_4^{3-}-P adsorption capacity ranged from about 0 to 30 mg/g for different biochar's that produced at 450°C and 650°C. Trazzi et al. (2016) investigated Sugar cane bagasse and Miscanthus giganteas biochar with different pyrolysis temperatures (between 300°C, 500°C and 700 °C) and two residence times of 20 or 60 minutes and conclude that phosphate adsorption on biochar's was endothermic and increased with process temperature. The amount of desorbed phosphate was proportional to its adsorption capacity. Concerning ammonium adsorption, the results are more significant in recent research. Liang et al. (2006) pointed out that high oxygen to carbon ratio could be responsible for nutrient adsorption, as well as, adsorption of ammonium on soluble organic matter on the surface of biochar is likely. Electrostatic interaction through cation or anion exchange to charged functional groups on biochar was suggested as governing mechanism of ammonium adsoprtion resulting pH-dependent adsorption process (Fidel et al., 2018, Yang et al., 2018). The maximum ammonium adsorption from slurry was 39.8 and 44.6 mg/g for wood and rice husk biochar respectively, as well as, adsorption increased with increase in contact time, temperature, pH and ammonium concentration but it decreased with increase in biochar particle size (Kizito et al., 2015). Similarly, Vu et al. (2017) found that ammonium adsorption on modified biochar strongly depended on pH. Desorption of ammonium was investigated at different pH environment which indicated less than 27% ammonium was desorbed in water (Wang et al., 2015b). Despite some studies have been carried out on biochar desorption, there is a lack of data about the effect of pH solution on ammonium and phosphate desorption.

The objectives of this study were to evaluate and compare the phosphate and ammonium adsorption capacity of biochar derived from woody biomass, as well as, to investigate the influence of biochar preparation conditions and pH environment on adsorption-desorption for phosphate and ammonium.

2. Material and method

2.1. Preparation of biochar

Pine wood chips were collected from a local carpenter in Tehran, Iran. In order to produce biochar, the wood source was initially dried at 80°C for 24 hours by oven, then wood feedstock was pyrolyzed at 400°C and 600°C with a heating rate of 5°C/min in a furnace under nitrogen gas for 60 and 120 minutes (Yao et al., 2012). Table 1 illustrates biochar samples and their production conditions. All biochar's sieved

to between 150 and 500 μm to obtain a uniform particle size.

Table 1. Production condition of biochar samples

Samples	*Temperature (°C)*	*Retention time (minute)*
BC1	400	60
BC2	400	120
BC3	600	60
BC4	600	120

2.2. Biochar characterization

Different parameters were studied to investigate the physical and chemical properties of biochar. Specific surface area of biochar was determined using Brunauer-Emmett-Teller (BET) technique (Sinha et al., 2019). Determination of volatile matter and ash content was performed in accordance with ASTM D1752-84. To measure the pH and electrical conductivity (EC) of biochar, 5 grams of biochar is stirred in 50 ml of distilled water, then wait 30 minutes to settle particles. Analysis is performed using a pH meter and EC meter (Singh et al., 2017). Elementary analysis of C/H/N was determined using a CHN Elemental Analyzer. The following formula is used to calculate the biochar yield (Eq. 1):

$$Yield\ (\%) = (biochar\ \ weight)/(dried\ biomass\ \ weight) \times 100 \quad (1)$$

The fixed carbon is measured using following Eq. (2):

$$Fixed\ Carbon\ (\%) = 100 - (percentage\ of\ ash + \\ + percentage\ of\ volatile\ matter) \quad (2)$$

2.3. Sorption experiment

Phosphate and ammonium solutions were prepared using NH_4Cl and K_2HPO_4. In order to obtain adsorption capacity of wood biochar's, batch-scale experiments were used for phosphate and ammonium solutions. First, all bottles were washed with 1 M HCl and then washed with distilled water. Four samples of biochar's (BC1, BC2, BC3, and BC4) were added to the bottle each weighing 0.1 g and then 100 ml of the solutions were added and the pH of the solutions were adjusted to 7 using NaOH. Phosphate adsorption capacity of four biochar's were measured in different concentrations of 5, 25, 50, 100, 250 and 500 mg/L. Similarly, different ammonium concentrations of 5, 50, 100, 250, 500 and 1000 mg/L were applied to investigate biochar adsorption capacity. In order to investigate pH effect on the phosphate adsorption capacity, 100 mg/L phosphate solution were applied and pH of the solutions were adjusted to 3, 5, 7, 9 and 11 using NaOH and HCl. For ammonium adsorption capacity, 100 mg/L concentration was used with pH of 3, 5, 7 and 9.

At pH>9, ammonium ions are increasingly converted to ammonia so pH=11 is not a good value. The cap of the bottle was fully tightened and stirred at 200 rpm for 24 hours at room temperature (25±0.5 °C). The output solution is centrifuged and filtered with filter paper and analysed using ultraviolet spectrophotometry. All experiments have been carried out in triplicate.

The amount of adsorbed ion on the biochar and the adsorption percentage are determined by the difference in initial concentration and equilibrium concentration. The amount of adsorption (q) and adsorption percentage (R) is calculated using Eqs. (3-4), where v denotes the volume of the solution (ml), m means the weight of biochar (g), C_0 and C_e denote the initial concentration and the equilibrium concentration of the ion (mg/L) respectively.

$$q = \frac{(C_0 - C_e)v}{m} \quad (3)$$

$$R = \frac{(C_0 - C_e)}{C_0} \times 100 \quad (4)$$

2.4. Adsorption isotherm

The adsorption isotherms are equations describing the adsorption equilibrium state between the solid and fluid phases. In this study, experimental data of adsorption equilibrium were investigated using Freundlich, Langmuir and Langmuir-Freundlich adsorption isotherm models. The Langmuir, Freundlich and Langmuir-Freundlich isotherms were applied to explain the adsorption of ammonium and phosphate to wood biochar's. These three isotherms are expressed as Eqs. (5-7), where Q_e is equilibrium amount of adsorbed matter (mg/g), C_e represents equilibrium concentration (mg/L), K_F,K_L and K_{LF} mean Freundlich, Langmuir and Langmuir-Freundlich isotherm constants respectively, 1/n is the heterogeneity factor., Q_{max} means maximum monolayer adsorption capacity (mg/g), Q_{MLF} means Langmuir-Freundlich maximum adsorption capacity (mg/g), M_{LF} is heterogeneous parameter and it lies between 0 and 1.

$$Q_e = K_F C_e^{1/n} \quad (5)$$

$$Q_e = Q_{\max} \frac{K_L C_e}{1 + K_L C_e} \quad (6)$$

$$Q_e = Q_{M_{LF}} \frac{(K_{LF} C_e)^{M_{LF}}}{1 + (K_{LF} C_e)^{M_{LF}}} \quad (7)$$

In order to evaluate the concordance of the results with the above isotherms, Linear equations are used. The linearized Freundlich, Langmuir and Langmuir-Freundlich using Eqs. (7-9):

$$Log\ Q_e = Log\ K_F + \frac{1}{n} Log\ C_e \quad (7)$$

$$\frac{1}{Q_e} = \left(\frac{1}{K_L\ Q_{\max}}\right)\frac{1}{C_e} + \frac{1}{Q_{\max}} \quad (8)$$

$$\frac{1}{Q_e} = \left(\frac{1}{K_{LF}{}^{M_{LF}} Q_{M_{LF}}}\right)\frac{1}{C_e{}^{M_{LF}}} + \frac{1}{Q_{M_{LF}}} \quad (9)$$

2.5. Desorption experiments

In order to measure desorption, 0.1 gram of BC2 and BC3 samples of biochar's were added to the bottle and then 100 ml of the ammonium and phosphate solutions were added with similar concentrations of adsorption experiments and the pH of the solutions were adjusted to 4 and 9 using NaOH and HCl. The lid of the bottle is fully tightened and stirred at room temperature (25±0.5 °C). for 200 rpm for 24 hours. The supernatant is centrifuged and filtered by ash less filter paper and then analysed. Distilled water was added to the remained biochar and the pH was adjusted to 7, then the solutions was stirred at 200 rpm for 24 hours at room temperature (25±0.5 °C). The supernatant is centrifuged and filtered with filter paper and finally analysed. All experiments have been carried out in triplicate. The desorption percentage is calculated based on the ratio of the desorbed nutrient to adsorbed nutrient (Eq. 10):

$$Desorption\ \ \% = (desorbed\ \ nutrient\ / \ / adsorbed\ \ nutrient\ ) \times 100 \quad (10)$$

2.6. Adsorption kinetics

In order to measure adsorption kinetics, 0.1 g of four samples of biochar's (BC1, BC2, BC3, and BC4) were added to 500 mg/L phosphate and 1000 mg/L ammonium as done in sorption experiment section. The cap of the bottle was fully tightened and stirred at 200 rpm for 0.5 h, 1 h, 2 h, 4 h, 8 h, 16 h, 24 h at room temperature (25 ± 0.5 °C). The output solution is centrifuged and filtered with filter paper and analyzed using ultraviolet spectrophotometry. All experiments have been carried out in triplicate. The adsorption kinetics of ammonium and phosphate are analyzed by the following kinetics Eqs. (11-13):

Pseudo-first-order $Q_t = Q_e(1 - e^{-k_1 t})$ (11)

Pseudo-second-order $Q_t = k_2 Q_e{}^2 t / (1 + k_2 Q_e t)$ (12)

Intraparticle diffusion $Q_t = k_3 t^{0.5} + C$ (13)

where: q_e and q_t (mg/g) are the adsorption capacity of biochar at the equilibrium time and at the given time, respectively; k_1 (h^{-1}), k_2 ($g.mg^{-1}.h^{-1}$) represent the rate constants of the three kinetic models; and C is a constant.

3. Results and discussion

3.1. Physicochemical properties of biochar

The Table 2 shows the parameters of pH, EC, specific surface area, biochar yield, ash content, volatiles and stabilized carbon. Elemental analysis of wood biochar's is presented in Table 3. The pH of the produced biochar's was above 7 and has a direct relationship with temperature and residence time. In addition, EC of biochar samples shows a similar trend. Li et al. (2013) investigated the mechanism of the effect of functional groups on the physicochemical properties of biochar which showed that the pH and EC of biochar depend on functional groups of different biomass feedstocks.

Therefore, these results show that increasing the temperature from 400 °C to 600 °C has a significant effect on the functional groups of biochar. According to Table 2 and Table 3, it can be concluded that for a specific biomass, higher pyrolysis temperatures and retention time resulted in lower biochar yield, higher pH, greater BET, higher EC, higher ash contents, lower carbon content, lower volatile matter and higher fixed carbon which is in line with the previous researches (Angın and Şensöz 2014; Rehrah et al., 2014; Zhao et al., 2017).

Table 2. Physicochemical properties of wood biochars

Sample	***Size (μm)***	***pH***	***EC (μS/cm)***	***BET (m^2/g^{-1})***	***Yield (%)***
BC1	150 - 500	7.80	31.3	0.7	40.46
BC2	150 - 500	8.01	33.4	0.9	35.42
BC3	150 - 500	8.84	38.5	57	36.75
BC4	150 - 500	9.02	41.3	95	28.64

Table 3. Elemental analysis of wood biochars

Sample	***C %***	***H %***	***N %***	***O %***	***Ash (%)***	***H/C***	***O/C***	***Volatile matter (%)***	***Fixed carbon (%)***
BC1	70.1	2.5	0.4	11.6	15.21	0.035	0.165	29.46	55.33
BC2	65.6	3.2	0.4	10.2	17.78	0.048	0.155	25.27	56.94
BC3	64.6	1.8	0.5	9.5	22.31	0.027	0.147	14.35	63.34
BC4	68.4	0.9	0.3	7.9	25.37	0.013	0.115	10.21	64.48

3.2. Phosphate and ammonium adsorption on biochar

The Fig. 1a shows the phosphate adsorption capacity by different biochar's at different concentrations. Phosphate adsorption capacities at concentration of 5 mg/L for BC1, BC2, BC3 and BC4 were 0.61, 0.75, 1.21 and 1.62 mg/g respectively. However, phosphate adsorption capacities for concentrations of 500 mg/L for BC1, BC2, BC3 and BC4 were14.90, 22.96, 35.53 and 42.26 mg/g, respectively. The Fig. 1a shows that adsorption capacity improved with increasing initial concentration which indicated that phosphate initial concentration could play an important role to overcome the mass transfer resistance between solution and biochar. The phosphate adsorption order of biochar's was BC4>BC3>BC2>BC1 at all concentrations. These results also indicate that the temperature and the retention time of the pyrolysis process had a significant positive effect on the phosphate adsorption capacity ($p < 0.05$) according to the result of ANOVA (analysis of variance) which is consistent with the study of Trazzi et al. (2016) that observed phosphate adsorption on biochar's increased with pyrolysis process temperature. Lower O/C ratio in higher temperature and retention time of pyrolysis process could limit ion exchange but the exponential growth of specific surface area can probably compensate this decrease. However, because of the tendency of biochar to be negatively charged, the surface performance does not affect adsorption mechanism significantly. Although the effect of specific surface area of biochar on phosphate adsorption is ambiguous, some studies have estimated this effect to be low compared to elemental uptake (Takaya et al., 2016). Wang et al. (2015a) found that biochar with the best adsorption performance did not have a higher surface area level than other biochar's, conversely the presence of functional groups had a positive effect on phosphate adsorption.

The Fig. 1b shows the ammonium adsorption by different biochar's at different concentrations. Ammonium adsorption capacities at concentration of 5 mg/L for BC1, BC2, BC3 and BC4 were0.92, 0.82, 0.73 and 0.34 mg/g, respectively. However, adsorption capacities for concentrations of 1000 mg/L for BC1, BC2, BC3 and BC4 were 5.30, 4.73, 4.13 and 2.05 mg/g, respectively. The Fig. 1b illustrates that adsorption capacities are obviously lower than the phosphate adsorption at all concentrations. Accordingly, BC1 showed highest adsorption percentage compared to other biochar's at all concentrations, while BC1 had lowest specific surface area which indicates that the surface area does not play a special role in ammonium adsorption. This result had already been observed by Hu et al., (2020). The ammonium adsorption order of biochar's was BC1>BC2>BC3>BC4 at all concentrations. These results also indicate that the temperature and the retention time of the pyrolysis process had a significant negative effect on the ammonium adsorption capacity ($p < 0.05$) according to the result of ANOVA (analysis of variance) which is in accordance with previous studies confirmed that adsorption of ammonium is maximized with lower pyrolysis temperatures (Fidel et al., 2018, Yang et al., 2018). BC1 had highest O/C ratio which means more oxygen-containing functional groups to cause better ammonium adsorption. Zeng et al. (2013) also showed that absence of aromatic functional groups at high temperatures reduces ammonium uptake. Furthermore, a direct relationship between functional groups and ammonium adsorption was observed in the study of Wang et al. (2015a). Zheng et al. (2014) also showed that with increasing pyrolysis temperature, ammonium adsorption decreased due to the lack of functional groups. Furthermore, ash content significantly increased with increasing temperature and retention time of pyrolysis process which was expected to have a negative effect on ammonium absorption.

The isotherm parameters of phosphate adsorption were obtained from Freundlich, Langmuir and Langmuir-Freundlich isotherms for different wood biochar's (Table 4). Based on the Coefficient of determination (R^2) value for phosphate adsorption it can be concluded that all three isotherms are in good agreement with the experimental results (R^2>0.9), but the Langmuir isotherm is more significantly consistent with R^2> 0.997 which means monolayer homogeneous phosphate adsorption at all of the binding sites.

Based on Langmuir isotherm, the maximum phosphate adsorption capacity is theoretically equal to 70.422 mg/g which is related to BC4, which was higher than previous studies (Park et al., 2015; Ren et al., 2015; Wang et al., 2016). For ammonium adsorption, the experimental results are more consistent with Freundlich and Langmuir-Freundlich isotherms than Langmuir isotherm which means the occurrence of chemical adsorption on heterogeneous surface. Based on Langmuir-Freundlich isotherm, maximum ammonium adsorption capacity could reach to 27.472 mg/g for BC1, which was slightly lower than Kizito et al., 2015 study.

3.3. Influence of adsorption pH

The effect of pH on phosphate adsorption was investigated. As shown in Fig. 2a for BC4, the highest phosphate adsorption efficiency (28.7%) was observed at pH = 3 and decreases with increasing pH so that the lowest adsorption (8.7%) occurred at pH = 11. The decrease in adsorption also occurred with increasing pH for the rest of biochar's. These results are consistent with Yin et al. (2018) study, which showed that phosphate adsorption on aluminium-modified biochar was pH-dependent and decreased with increasing pH. At low pH the adsorbent has a positive ion, which facilitates the adsorption of negative ions such as phosphate. However, at high pH, the OH^- ion competes with the phosphate ion for adsorption at the adsorption sites (Olgun et al., 2013).

The effect of pH on ammonium adsorption was investigated. In pH > 9 ammonium ions are converted to ammonia which obscures the adsorption mechanism. Fig. 2b shows that highest ammonium adsorption was occurred at pH =7 and reducing with decreasing pH accordingly lowest adsorption occurred at pH 3. These results are consistent with Fidel et al. (2018), Kizito et al. (2015) and Khalil et al. (2018), which showed that in an acidic environment, H^+ ions compete with ammonium ions, and thus the adsorption percentage reduces with decreasing pH which indicates ammonium adsorption is a pH-dependent reaction. Furthermore, in lower pH, positively charged functional groups on the biochar surfaces could limit the polar attraction of ammonium ions (Khalil et al., 2018).

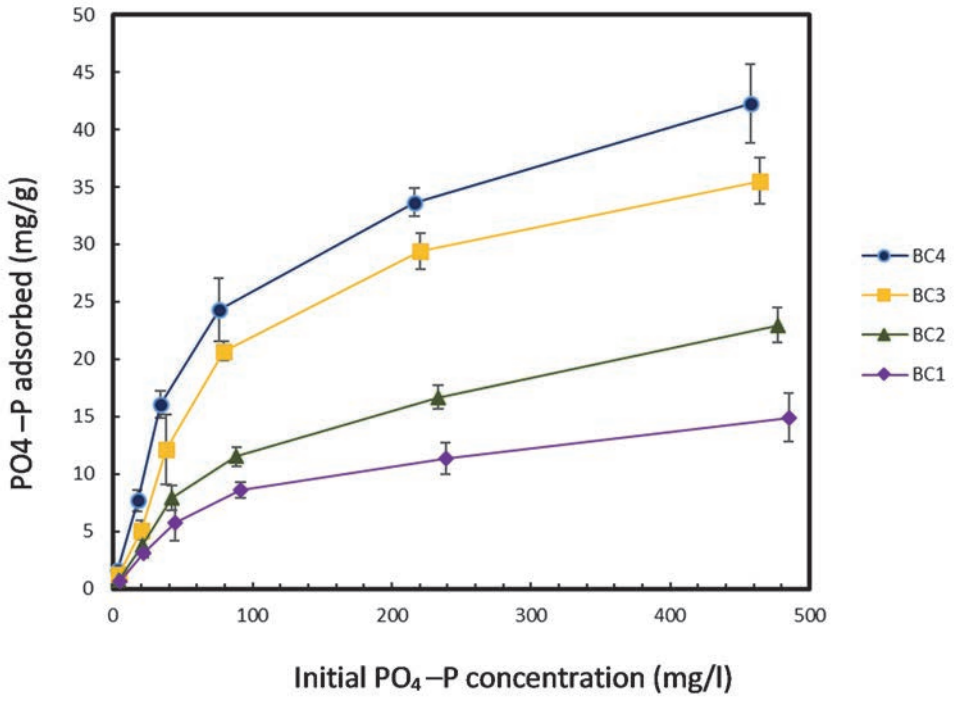

(a)

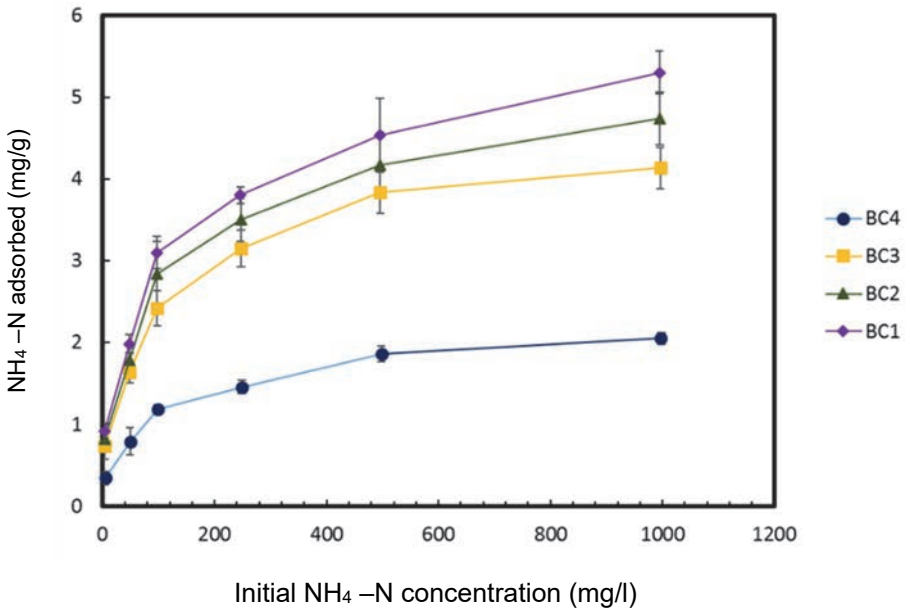

(b)

Fig. 1. Phosphate and ammonium adsorption at different concentrations: (a) phosphate adsorption, (b) ammonium adsorption

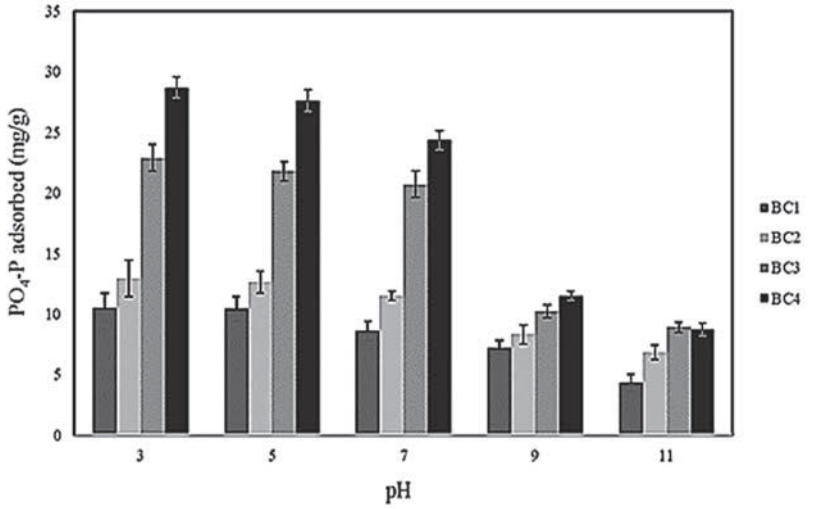

(a)

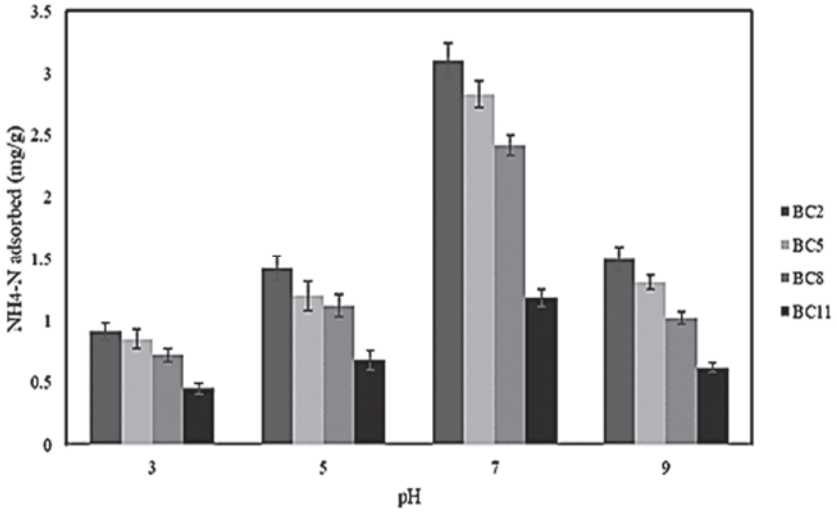

(b)

Fig. 2. Effect of pH on phosphate and ammonium adsorption of wood biochar's:
(a) phosphate adsorption, (b) ammonium adsorption

Table 4. Coefficient of determination (R^2) and model parameters for Langmuir, Freundlich and Langmuir-Freundlich isotherms for phosphate and ammonium adsorption on different wood biochar's at 25°C

Biochar adsorbent	***Adsorbate***	***Freundlich***			***Langmuir***			***Langmuir-Freundlich***			
		K_F	n	R^2	Q_{max}	K_L	R^2	Q_{MLF}	K_{LF}	M_{LF}	R^2
BC1	PO_4^{3-}	0.991	2.262	0.961	27.932	0.005	0.998	17.412	0.0071	1	0.952
	NH_4^{1+}	0.735	3.448	0.973	3.677	0.079	0.935	27.472	2.5E-05	0.367	0.993
BC2	PO_4^{3-}	1.133	6.706	0.976	54.945	0.003	0.998	29.922	0.0053	1	0.966
	NH_4^{1+}	0.681	3.496	0.964	3.339	0.076	0.935	24.570	2.7E-05	0.372	0.993
BC3	PO_4^{3-}	2.275	2.188	0.931	49.925	0.006	0.997	92.592	0.0034	0.935	0.995
	NH_4^{1+}	0.611	3.508	0.971	3.017	0.070	0.948	13.563	0.00018	0.406	0.996
BC4	PO_4^{3-}	3.294	2.364	0.949	70.422	0.007	0.999	50/581	0.009	1	0.991
	NH_4^{1+}	0.275	2.512	0.968	1.469	0.061	0.952	6.180	0.00025	0.427	0.996

3.3. Adsorption kinetics

In order to better understand the adsorption mechanism and effect of adsorption time, adsorption kinetic experiments were conducted. Three kinetic models were applied to compare and analyze the results illustrated in Fig. 3.

According to the results, the adsorption can be divided into two stages. In the first stage, both ammonium and phosphate are rapidly adsorbed on the biochar, so that at least 80% of the 24-hour maximum absorption capacity is adsorbed within 4 hours for all samples which could be attributed to several fresh adsorption sites on the biochar surface. In the second

stage, the adsorption is significantly slowed down and gradually increasing to the equilibrium adsorption amount.

Table 5 shows that both pseudo-first-order and pseudo-second-order are optimal models to predict the adsorption kinetics of phosphate and ammonium. This result indicates that the chemical adsorption could be considered as the major machanism for phosphate and ammonium absorption which is in good agreement with recent studies (Khalil et al., 2018, Wang et al., 2016; Yin et al., 2018).

Intraparticle diffusion was not suitable model with R^2 values lower than 0.80 for all biochar samples, which indicated that external and internal diffusions are limiting factors in phosphate and ammonium absorption (Yin et al., 2018).

3.4. Phosphate desorption

Fig. 4a shows the desorption rate for two biochar's (BC2 and BC3) for pH = 4 and pH = 9. Accordingly, the amount of phosphate desorbed is directly related to the amount of phosphate initially absorbed. As well as, pH has a clear effect on the amount of desorbed so that at pH=9 the phosphate desorption is clearly higher than pH = 4, this can be attributed to the competition of OH^- ions with phosphate anions.

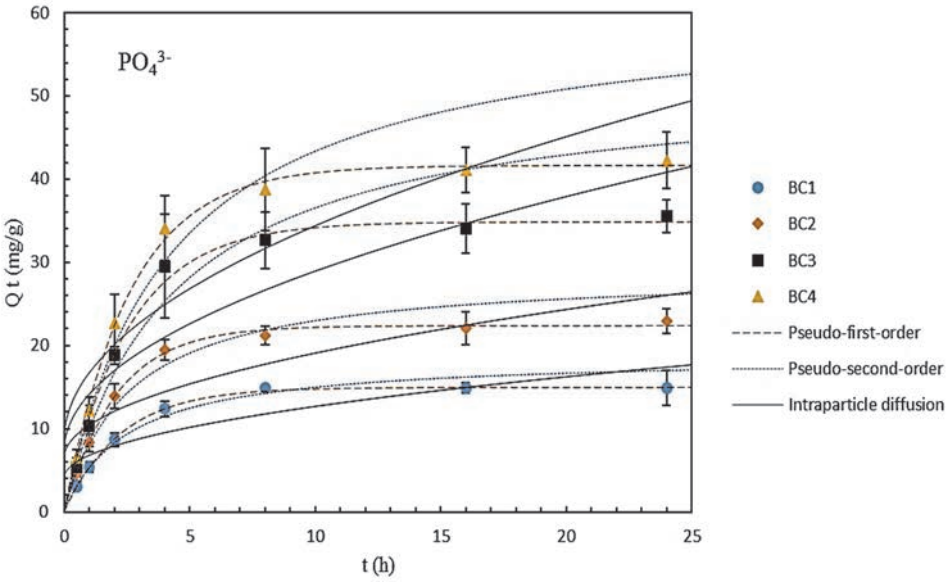

(a)

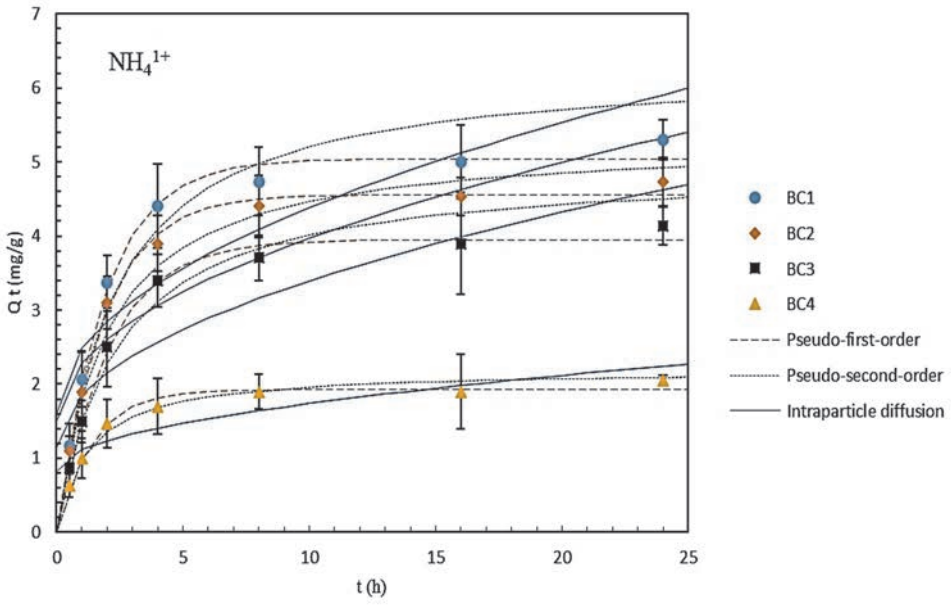

(b)

Fig. 3. Adsorption kinetics of phosphate and ammonium on biochar: (a) phosphate adsorption (b) ammonium adsorption

Phosphate desorption percentage at pH = 9 was between 56% and 89%, whereas phosphate desorption percentage at pH = 4 varied from 22% to 67%. Fig. 4b shows the ammonium desorption for two biochar's (BC2 and BC3) in two pH = 4 and pH = 9. The ammonium desorption is directly related to the initially absorbed ammonium. The results indicated that pH plays an important role in ammonium desorption on biochar. In pH=4 the existing H^+ ions in solution compete with adsorbed ammonium ions and accelerate the desorption process.

Ammonium desorption percentage at pH = 9 was between 13% and 23%, whereas ammonium desorption percentage at pH = 4 varied from 29% to 40% which is in good agreement with Wang et al. (2015b).

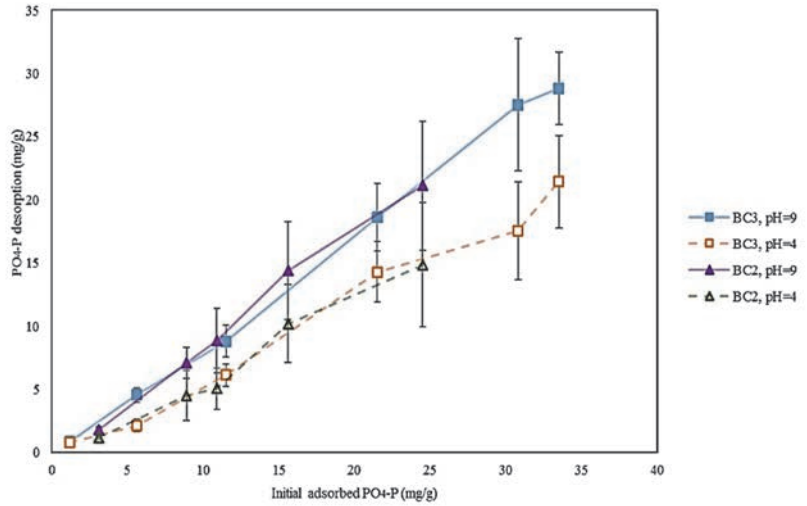

(a)

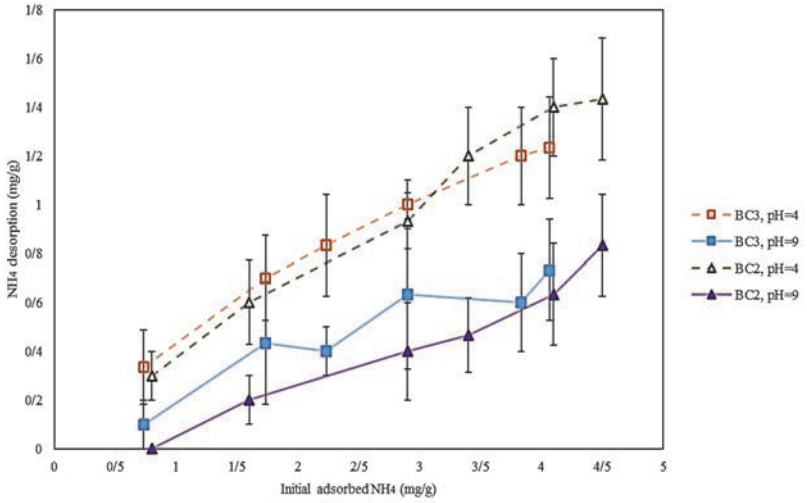

(b)

Fig. 4. Desorption of phosphate and ammonium on biochar's at pH = 4 and pH = 9: (a) phosphate adsorption, (b) ammonium adsorption

Table 5. Parameters of phosphate and ammonium adsorption kinetics

Biochar adsorbent	*Adsorbate*	*Pseudo-first-order*			*Pseudo-second-order*			*Intraparticle diffusion*		
		Q_e	k_1	R^2	Q_e	k_2	R^2	k_3	C	R^2
BC1	PO_4^{3-}	14.997	0.441	0.998	18.761	0.021	0.997	2.718	4.046	0.758
	NH_4^{1+}	5.041	0.530	0.991	2.198	0.373	0.995	0.879	1.602	0.770
BC2	PO_4^{3-}	22.325	0.481	0.996	28.902	0.013	0.994	4.015	6.403	0.761
	NH_4^{1+}	4.559	0.539	0.994	4.941	0.087	0.995	0.780	1.502	0.762
BC3	PO_4^{3-}	34.896	0.394	0.992	52.08	0.004	0.992	6.836	7.303	0.777
	NH_4^{1+}	3.950	0.486	0.993	5.612	0.88	0.994	0.711	1.144	0.782
BC4	PO_4^{3-}	41.622	0.385	0.995	61.349	0.004	0.993	8.199	8.480	0.792
	NH_4^{1+}	1.925	0.716	0.979	6.325	0.073	0.993	0.288	0.827	0.747

4. Conclusions

This study investigated the mechanisms of nutrient adsorption and desorption on biochar. The phosphate and ammonium adsorption capacities of biochar have evaluated and compared, as well as, the effect of biochar preparation conditions on adsorption-desorption capacity investigated for phosphate and ammonium. For different biochar's, ammonium adsorption capacity was about 0.34 to 5.30 mg/g and phosphate adsorption capacity were about 0.6 to 42.2 mg/g. Experimental results illustrated that phosphate adsorption capacity are strongly related to temperature and retention time of pyrolysis process.

However, higher ammonium adsorption was occurred in lower pyrolysis temperature and residence time which means oxygen-containing functional groups is probably one of the main effective factors. In addition, although phosphate and ammonium adsorptions are pH-dependent, the phosphate adsorption significantly reduced with increasing pH solution whereas for ammonium the highest adsorption occurred in neutral condition (pH=7). Results of adsorption kinetics indicated that both pseudo-first-order and pseudo-second-order are optimal models to predict the adsorption kinetics concluding that the chemical adsorption could be considered as major mechanisms for phosphate and ammonium absorption. According to the results of possible adsorption-desorption mechanisms, it can be concluded that both phosphate and ammonium adsorptions and desorption's are significantly affected by pH environment which is in line with previous studies, but some characteristics of biochar such as specific surface area and yield have no justifiable effect on the adsorption process which requires more extensive studies.

References

Al Arni S., (2018), Comparison of slow and fast pyrolysis for converting biomass into fuel, *Renewable Energy*, **124**, 197-201.

Alhashimi H.A., Aktas C.B., (2017), Life cycle environmental and economic performance of biochar compared with activated carbon: a meta-analysis, *Resources*, *Conservation and Recycling*, **118**, 13-26.

Angın D., Şensöz S., (2014), Effect of pyrolysis temperature on chemical and surface properties of biochar of rapeseed (Brassica napus L.), *International Journal of Phytoremediation*, **16**, 684-693.

Balat M., Balat M., Kırtay E., Balat H., (2009), Main routes for the thermo-conversion of biomass into fuels and chemicals. Part 1: Pyrolysis systems, *Energy Conversion and Management*, **50**, 3147-3157.

Fagbohungbe M.O., Herbert B.M., Hurst L., Ibeto C.N., Li H., Usmani S.Q., Semple K.T., (2017), The challenges of anaerobic digestion and the role of biochar in optimizing anaerobic digestion, *Waste Management*, **61**, 236-249.

Fidel R.B., Laird D.A., Spokas K.A., (2018), Sorption of ammonium and nitrate to biochars is electrostatic and pH-dependent, *Scientific Reports*, **8**, 17627, doi: 10.1038/s41598-018-35534-w

Hollister C.C., Bisogni J.J., Lehmann J., (2013), Ammonium, nitrate, and phosphate sorption to and solute leaching from biochars prepared from corn stover (Zea mays L.) and oak wood (Quercus spp.), *Journal of Environmental Quality*, **42**, 137-144.

Hu X., Zhang X., Ngo H.H., Guo W., Wen H., Li C., Zhang Y., Ma C., (2020), Comparison study on the ammonium adsorption of the biochars derived from different kinds of fruit peel, *Science of the Total Environment*, **707**, 135544, doi: 10.1016/j.scitotenv.2019.135544

Huggins T.M., Haeger A., Biffinger J.C., Ren Z.J., (2016), Granular biochar compared with activated carbon for wastewater treatment and resource recovery, *Water Research*, **94**, 225-232.

Jackson R.W., Neto A.B.F., Erfanian E., (2018), Woody biomass processing: Potential economic impacts on rural regions, *Energy Policy*, **115**, 66-77.

Kan T., Strezov V., Evans T.J., (2016), Lignocellulosic biomass pyrolysis: A review of product properties and effects of pyrolysis parameters, *Renewable and Sustainable Energy Reviews*, **57**, 1126-1140.

Khalil A., Sergeevich N., Borisova V., (2018), Removal of ammonium from fish farms by biochar obtained from rice straw: Isotherm and kinetic studies for ammonium adsorption, *Adsorption Science & Technology*, **36**, 1294-1309.

Kizito S., Wu, S., Kirui W.K., Lei M., Lu Q., Bah H., Dong R., (2015), Evaluation of slow pyrolyzed wood and rice husks biochar for adsorption of ammonium nitrogen from piggery manure anaerobic digestate slurry, *Science of the Total Environment*, **505**, 102-112.

Laird D., Fleming P., Wang B., Horton R., Karlen D., (2010), Biochar impact on nutrient leaching from a Midwestern agricultural soil, *Geoderma*, **158**, 436-442.

Lehmann J., Joseph S., (2015), *Biochar for Environmental Management: An Introduction*, In: *Biochar for Environmental Management: Science, Technology and Implementation*, 2nd Edition, Routledge, New York, 1-14.

Li X., Shen Q., Zhang D., Mei X., Ran W., Xu Y., Yu G., (2013), Functional groups determine biochar properties (pH and EC) as studied by two-dimensional 13C NMR correlation spectroscopy, *PLoS One*, **8**, 65949, doi:10.1371/journal.pone.0065949.

Liang B., Lehmann J., Solomon D., Kinyangi J., Grossman J., O'neill B., Skjemstad J.O., Thies J., Luizão F.J., Petersen J., Neves E.G., (2006), Black carbon increases cation exchange capacity in soils, *Soil Science Society of America Journal*, **70**, 1719-1730.

Liikanen M., Grönman K., Deviatkin I., Havukainen J., Hyvärinen M., Kärki T., Varis J., Soukka R., Horttanainen M., (2019), Construction and demolition waste as a raw material for wood polymer composites–Assessment of environmental impacts, *Journal of Cleaner Production*, **225**, 716-727.

McCarl B.A., Peacocke C., Chrisman R., Kung C.C., Sands R.D., (2009), *Economic Evaluation of Biochar Systems: Current Evidence and Challenges*, In: *Biochar for Environmental Management: Science*, *Technology and Implementation*, Lehmann J., Joseph S. (Eds.), 2nd Edition, Routledge, New York, 813-852.

Novais S.V., Zenero M.D.O., Barreto M.S.C., Montes C.R., Cerri C.E.P., (2018), Phosphorus removal from eutrophic water using modified biochar, *Science of the Total Environment*, **633**, 825-835.

Olgun A., Atar N., Wang S., (2013), Batch and column studies of phosphate and nitrate adsorption on waste

solids containing boron impurity, *Chemical Engineering Journal*, **222**, 108-119.

Oliveira F.R., Patel A.K., Jaisi D.P., Adhikari S., Lu H., Khanal S.K., (2017), Environmental application of biochar: Current status and perspectives, *Bioresource Technology*, **246**, 110-122.

Paolotti L., Martino G., Marchini A., Boggia A., (2017), Economic and environmental assessment of agro-energy wood biomass supply chains, *Biomass and Bioenergy*, **97**, 172-185.

Park J.H., Ok Y. S., Kim S.H., Cho J.S., Heo J.S., Delaune R.D., Seo D.C., (2015), Evaluation of phosphorus adsorption capacity of sesame straw biochar on aqueous solution: influence of activation methods and pyrolysis temperatures, *Environmental Geochemistry and Health*, **37**, 969-983.

Peng X.Y.L.L., Ye L.L., Wang C.H., Zhou H., Sun B., (2011), Temperature-and duration-dependent rice straw-derived biochar: Characteristics and its effects on soil properties of an Ultisol in southern China, *Soil and Tillage Research*, **112**, 159-166.

Rehrah D., Reddy M.R., Novak J.M., Bansode R.R., Schimmel K.A., Yu J., Watts D.W., Ahmedna M., (2014), Production and characterization of biochars from agricultural by-products for use in soil quality enhancement, *Journal of Analytical and Applied Pyrolysis*, **108**, 301-309.

Ren J., Li N., Li L., An J.K., Zhao L., Ren, N.Q., (2015), Granulation and ferric oxides loading enable biochar derived from cotton stalk to remove phosphate from water. *Bioresource Technology*, **178**, 119-125.

Shareef T.M.E., Zhao B., (2017), The Fundamentals of Biochar as a Soil Amendment Tool and Management in Agriculture Scope: An Overview for Farmers and Gardeners, *Journal of Agricultural Chemistry and Environment*, **6**, 38-61.

Singh B., Dolk M.M., Shen Q., Camps-Arbestain M., (2017), *Biochar pH*, *Electrical Conductivity and Liming Potential*, In: *Biochar: A Guide to Analytical Methods*, Singh B., Camps-Arbestain M., Lehmann J. (Eds.), Csiro Publishing, Clayton, Australia, 23-38.

Sinha P., Datar A., Jeong C., Deng X., Chung Y. G., Lin, L. C., (2019), Surface area determination of porous materials using the Brunauer–Emmett–Teller (BET) method: limitations and improvements, *The Journal of Physical Chemistry C: Energy*, *Materials*, *and Catalysis*, **123**, 20195-20209.

Takaya C.A., Fletcher L.A., Singh S., Anyikude K U., Ross A.B., (2016), Phosphate and ammonium sorption capacity of biochar and hydrochar from different wastes, *Chemosphere*, **145**, 518-527.

Tan X., Liu Y., Zeng G., Wang X., Hu X., Gu Y., Yang Z., (2015), Application of biochar for the removal of pollutants from aqueous solutions, *Chemosphere*, **125**, 70-85.

Tang J., Zhu W., Kookana R., Katayama A., (2013), Characteristics of biochar and its application in remediation of contaminated soil, *Journal of Bioscience and Bioengineering*, **116**, 653-659.

Trazzi P.A., Leahy J.J., Hayes M.H., Kwapinski W., (2016), Adsorption and desorption of phosphate on biochars, *Journal of Environmental Chemical Engineering*, **4**, 37-46.

Vu T.M., Doan D.P., Van H.T., Nguyen T.V., Vigneswaran S., Ngo H.H., (2017), Removing ammonium from water using modified corncob-biochar, *Science of the Total Environment*, **579**, 612-619.

Wang Z., Guo H., Shen F., Yang G., Zhang Y., Zeng Y., Wang L., Xiao H., Deng S., (2015a), Biochar produced from oak sawdust by Lanthanum (La)-involved pyrolysis for adsorption of ammonium (NH_4^+), nitrate (NO_3^-), and phosphate (PO_4^{3-}), *Chemosphere*, **119**, 646-653.

Wang B., Lehmann J., Hanley K., Hestrin R., Enders, A., (2015b) Adsorption and desorption of ammonium by maple wood biochar as a function of oxidation and pH, *Chemosphere*, **138**, 120-126.

Wang Z., Shen D., Shen F., Li T., (2016), Phosphate adsorption on lanthanum loaded biochar, *Chemosphere*, **150**, 1-7.

Wei J., Tu C., Yuan G., Bi D., Wang H., Zhang L., Theng B.K., (2019), Pyrolysis temperature-dependent changes in the characteristics of biochar-borne dissolved organic matter and its copper binding properties, *Bulletin of Environmental Contamination and Toxicology*, **103**, 169-174.

Weber K., Quicker P., (2018), Properties of biochar, *Fuel*, **217**, 240-261.

Yang H.I., Lou K., Rajapaksha A.U., Ok Y.S., Anyia A.O., Chang S.X., (2018), Adsorption of ammonium in aqueous solutions by pine sawdust and wheat straw biochars, *Environmental Science and Pollution Research*, **25**, 25638-25647.

Yao Y., Gao B., Zhang M., Inyang M., and Zimmerman A. R., (2012), Effect of biochar amendment on sorption and leaching of nitrate, ammonium, and phosphate in a sandy soil, *Chemosphere*, **89**, 1467-1471.

Yin Q., Ren H., Wang R., Zhao Z., (2018), Evaluation of nitrate and phosphate adsorption on Al-modified biochar: Influence of Al content, *Science of The Total Environment*, **631**, 895-903.

Zeng Z., Li T.Q., Zhao F.L., He Z.L., Zhao H.P., Yang X.E., Wang H., Zhao J., Rafiq M.T., (2013), Sorption of ammonium and phosphate from aqueous solution by biochar derived from phytoremediation plants, *Journal of Zhejiang University Science B: Biomedicine & Biotechnology*, **14**, 1152-1161.

Zhang H., Chen C., Gray E.M., Boyd S.E., Yang H., Zhang D., (2016), Roles of biochar in improving phosphorus availability in soils: a phosphate adsorbent and a source of available phosphorus, *Geoderma*, **276**, 1-6.

Zhao B., O'Connor D., Zhang J., Peng T., Shen Z., Tsang D.C., Hou D., (2018), Effect of pyrolysis temperature, heating rate, and residence time on rapeseed stem derived biochar, *Journal of Cleaner Production*, **174**, 977-987.

Zhao S.X., Ta N., Wang X.D., (2017), Effect of temperature on the structural and physicochemical properties of biochar with apple tree branches as feedstock material, *Energies*, **10**, 1293, doi: 10.3390/en10091293.

Zheng Y., Yu Q., Wang H., Wang Y., He N., Shen L., Li Q., (2014), Preparation of biochars from biogas residue and adsorption of ammonia-nitrogen in biogas slurry, *CIESC Journal*, **65**, 1856-1861.

Zhou Z., Xu Z., Feng Q., Yao D., Yu J., Wang D., Lv S., Liu Y., Zhou N.. Zhong M.E., (2018), Effect of pyrolysis condition on the adsorption mechanism of lead, cadmium and copper on tobacco stem biochar, *Journal of Cleaner Production*, **187**, 996-1005.

Zhu N., Yan T., Qiao J., Cao H., (2016), Adsorption of arsenic, phosphorus and chromium by bismuth impregnated biochar: Adsorption mechanism and depleted adsorbent utilization, *Chemosphere*, **164**, 32-40.